

Article

Influence of Non-Invasive Zirconium Oxide Surface Treatment on Phase Changes

Kinga Regulska , Bartłomiej Januszewicz , Anna Jędrzejczak  and Leszek Klimek * 

Institute of Materials Science and Engineering, Faculty of Mechanical Engineering, Lodz University of Technology, Stefanowskiego 1/15, 90-537 Lodz, Poland; kinga.regulska@dokt.p.lodz.pl (K.R.); bartlomiej.januszewicz@p.lodz.pl (B.J.); anna.jedrzejczak@p.lodz.pl (A.J.)

* Correspondence: leszek.klimek@p.lodz.pl

Abstract: The aim of the research was to find a zirconia treatment method that would reduce or minimize the transformation from the tetragonal phase to the monoclinic phase. Background: Yttria-stabilized zirconia is increasingly chosen for the base of permanent prosthetic restorations. To achieve a good bond between the prosthetic cup and the veneer material, the material must be treated to achieve surface development. This is a mechanical process, during which an unfavorable transformation from the tetragonal into the monoclinic phase takes place, which leads to the weakening of the internal structure of zirconium dioxide, and later damages the prosthetic restoration. Methods: The tested material consisted of cylindrical samples of 3Y-TZP CeramillZi zirconium oxide, which were sintered after cutting out from the block. After sintering, the samples were subjected to the following types of processing: laser structuring, chemical etching and plasma etching. After the surface treatments, the samples were subjected to diffraction tests to determine the phase composition. Next, the wettability was tested to determine the surface free energy. Results: On the basis of the conducted tests, it was noticed that the applied treatments caused a phase transformation from the tetragonal to the monoclinic phase. After the process of chemical etching, the range of the monoclinic phase for the sample was 5%; after plasma etching, it was 8%, and after laser structuring, it was 2%. In addition, post-surface free energy studies have shown that zirconia is wetted better with an apolar than a polar liquid. Conclusions: The obtained results indicate that the transformation was minimized with the treatments we applied; that is why they are called non-invasive methods. According to the literature data, depending on the parameters of the sandblasting process, the percentage of the monoclinic phase in the treated surfaces ranges from 22% to 52%, which confirms the above-mentioned conclusion.

Keywords: zirconia; prosthetics; transformation; treatment; etching; laser; structuring



Citation: Regulska, K.; Januszewicz, B.; Jędrzejczak, A.; Klimek, L. Influence of Non-Invasive Zirconium Oxide Surface Treatment on Phase Changes. *Ceramics* **2024**, *7*, 222–234. <https://doi.org/10.3390/ceramics7010014>

Academic Editor: Angel L. Ortiz

Received: 11 December 2023

Revised: 21 January 2024

Accepted: 29 January 2024

Published: 8 February 2024



Copyright: © 2024 by the authors. Licensee MDPI, Basel, Switzerland. This article is an open access article distributed under the terms and conditions of the Creative Commons Attribution (CC BY) license (<https://creativecommons.org/licenses/by/4.0/>).

1. Introduction

Recently, patient's awareness of oral health and hygiene has been increasing. More often they reach for modern solutions in the field of dental prosthetics. Crowns and prosthetic bridges are restorations that rebuild one tooth or several teeth, which is why patients seek these treatments only for health reasons. Sometimes, they play an aesthetic role, leveling certain imperfections in the smile. Zirconia is gaining popularity as a base material for permanent prosthetic restorations. It is primarily a highly aesthetic material due to its bright color, which is why it has displaced traditional metal alloys. It is primarily biocompatible and characterized by high-strength properties. However, it has disadvantages—it is a brittle material, so exceptional care should be taken when working with it [1–5]. The KIC cracking strength of the material is about $10 \text{ MPa}\cdot\text{m}^{1/2}$, the tensile strength is 330 MPa, the bending strength is 1000–1400 MPa, and the compressive strength is about 2000 MPa [6,7].

Zirconia exists in three structural varieties: monoclinic α -ZrO₂, tetragonal β -ZrO₂ and cubic γ -ZrO₂. The monoclinic form is stable at low temperatures—heating it to about

1170 °C leads to a transition to the tetragonal form, which is favorable from the point of view of biomechanics, and it is stable to about 2370 °C. At this temperature, there is a transition to the regular variety, which melts at 2680 °C. When the tetragonal form is cooled to a temperature of about 1000 °C, a reversible transformation into the monoclinic form takes place, along with the associated decrease in density and increase in volume.

The phase transformation from the tetragonal into the monoclinic phase may also occur when the material is subjected to diverse types of stimuli, such as chewing force, exposure to water, temperature changes, pH changes and various types of organisms existing in the oral cavity [8].

In dental prosthetics, sintered zirconium oxide with a grain size of 0.2–0.5 µm and a tetragonal structure is used. To preserve this structure at ambient temperatures, ZrO₂ is stabilized with magnesium, calcium, yttrium and cerium oxides [7,9–13]. Compared with other stabilizers, the solubility of yttrium in zirconium oxide is higher. Thanks to this, the grains gain greater stability before the phase transition from the tetragonal phase to the monoclinic phase, making it possible to produce a material containing 100% of the tetragonal phase. Moreover, yttrium is the most effective additive because it provides high-quality bond strength to the veneering material [14].

Ceramics based on zirconium oxide used for dental purposes have a metastable tetragonal form, partially stabilized at room temperature. This metastability means that there is still trapped energy inside the material, causing it to return to the monoclinic phase. Additionally, when surface treatments are applied, heat and energy are supplied to the material, initiating the occurrence of a phase transformation [11].

Zirconium oxide substructures are fabricated using CAD/CAM methods. Ready, pre-sintered blocks are milled to make the final prosthetic restoration and then sintered at temperatures of 1450 °C. This method allows a marginal seal of 30 µm to be obtained for the restoration, which is a satisfactory value. Please note that clinically acceptable marginal seals for prosthetic restorations are 100 µm. Thanks to this, ZrO₂ can be classified as one of the most aesthetic and durable materials for use in the oral cavity because, thanks to such perfect tightness, the risk of cementation or other defects occurring primarily at the cervix is negligible [11,15,16].

The surface roughness can be divided into three categories: macro, micro and nano. For prosthetic restorations and implants, the roughness usually covers the micro scale from 1 to 10 µm. A change in roughness can be achieved using various surface treatment methods for the material [17].

To achieve a good bond between the framework and the veneering material, the surface of the material must be modified. The surface treatment of the material plays a key role when it comes to the zirconia-veneering material bond. The most common are mechanical treatments such as grinding and sandblasting [18]. However, these methods are invasive and cause an unfavorable transformation from the tetragonal phase to the monoclinic one, which, in turn, reduces the durability of the restoration, causing the chipping and cracking of the facing material during the use of the prosthesis. According to the literature data, depending on the parameters of the sandblasting process, the percentage of the monoclinic phase in the treated surfaces ranges from 22% to 52%. After the grinding process which involves the use of diverse types of abrasives, it is in the range of 5–16% [1,19,20]. The tetragonal phase and the monoclinic phase differ in specific volume, so stresses are generated during the transformation that may cause the destruction of the material. The monoclinic phase is a stable phase at ambient temperature, while the tetragonal phase is metastable. Providing energy during mechanical processes activates the transformation from a metastable tetragonal phase into a stable monoclinic. Due to the high chemical resistance of zirconium oxide, it is not possible to create surface layers that facilitate the bonding of ceramics to the substrate, as in the case of Co-Cr or Ni-Cr alloys. Therefore, the only method to improve adhesion is to develop the surface and provide the possibility of mechanical attachments of the flowing liquid ceramic into the surface irregularities

resulting from surface treatment. In view of the above, the most frequently used method of surface processing is abrasive blasting, which causes irregularities in the treated surface.

Currently, less aggressive processing methods are being sought, which, on the one hand, will allow for structuring the surface and, on the other hand, will minimize the degree of tetragonal to monoclinic transformation.

One of the methods that can lead to surface development is chemical etching with acids. It is intended to contribute to increasing the roughness of the material surface [21–24]. Etching can be carried out in an acidic or alkaline environment [25,26]. Prosthetic recommendations recommend 5% or 9.5% hydrofluoric acid [27,28]. However, the effects of these processes turn out to be unsatisfactory; the differences in roughness before and after etching range within a dozen or so nanometers [21]. Crystalline ceramics are resistant to etching because they do not contain a glassy phase; therefore, it seems advisable to use stronger etchants [29]. In other applications, strong acid solutions are recommended, e.g., 45% HF, a mixture of 98% H₂SO₄, and 65% HNO₃ at a volume ratio of 1:3. The effects of the etching process depend on the type of etching agent, exposure time and its concentration. However, effective etching of the ceramic surface is considered a major step in direct ceramic repair during clinical management.

Another method that can be considered is plasma etching. Two phenomena are possible during this process: physical sputtering of the substrate material by plasma ions and chemical sputtering, based on fluorine radicals, which form volatile compounds with the substrate material and are removed from the reactor. Selective material removal is initially used in the production of very large-scale integrated circuits to define thin patterns, [30,31]. If part of the surface of the etched material is properly masked before the process, it is possible to model three-dimensional structures.

During the laser structuring process, regularly ordered geometric shapes are created on the surface by means of laser radiation (usually the pulsed one). The material is melted in a controlled manner using a laser beam and evaporated (ablation) or solidified in a defined structure. Due to the fact that the beam can cover even small areas and it is possible to control the amount of transmitted energy, it is possible to modify the surface to a large extent. Considering the high chemical resistance of zirconium oxide, surface development by producing microstructures on its surface should improve the adhesion of the material with veneering ceramics [32].

Traditional and commonly used methods of removing material from the surface include grinding, polishing and sandblasting processes. Our earlier research proved that the phase transformation from the tetragonal phase to the monoclinic one occurs to a significant extent [1,19]. Other methods, such as chemical etching, plasma etching, and laser structuring, can significantly contribute to reducing its quantity and thus improve the quality of future prosthetic restorations. These are new methods within the context of their application in prosthetic and dental offices and can be a particularly viable alternative to those currently used. Moreover, their influence on the phase structure of the zirconium oxide has not been studied and compared so far in the world literature.

The aim of the research presented in this paper was to find a zirconia treatment method that would minimize the transition from the tetragonal phase to the monoclinic one as much as possible while obtaining parameters characterizing the surface at a level ensuring proper bonding of the zirconia substructure with the veneering ceramics. They are called non-invasive methods because they do not cause a significant phase transformation from the tetragonal to the monoclinic phase.

2. Materials and Methods

The studied material consisted of cylindrical samples of 3Y-TZP CeramillZi zirconium oxide (Shenzhen Upcera Dental Technology, Shenzhen, China), which, after cutting out of the block, were mechanically polished and then were sintered in a furnace (CeramillTherm, Koblach, Austria) in the universal program (8°/min from 200 °C to 1450 °C, 2 h at a constant temperature of 1450 °C). The whole sintering process took about 10 h. The

shrinkage of the material was approximately 21%. After sintering, the samples had the following dimensions: a diameter of 20 and a height of 10 mm.

The sintered samples were subjected to the following types of treatment: chemical etching, plasma etching and laser structuring. The reference sample was a milled sample. Three samples were made for each test group.

Processing parameters

Chemical etching was conducted by immersing the sample in 40% HF for 30 min. The solution was at room temperature. The sample was then removed, rinsed with distilled water and dried using compressed air.

The dry etching process in the plasma of the ceramic surface was carried out using SF₆ gas (sulfur hexafluoride, 5.0, Linde). The following process parameters were applied in the modification: a substrate bias voltage of −600 V, a pressure of 4.5 Pa and an SF₆ gas flow rate of 10 sccm. During the etching process, a mask made of stainless steel (AISI 304) in the form of a woven wire mesh with an aperture size of 35 μm and wire diameter of 30 μm was present on the surface. As a result, after the etching process in plasma, a mask geometry was mapped on the modified surface and the etched structures sized according to the mask aperture were created. The etching process in SF₆ plasma lasted 60 min and was performed in a reactor (Alcatel No. 257, Paris, France) used for the deposition of thin films by the RF PECVD (radiofrequency plasma-enhanced chemical vapor deposition) method. The surface morphology of the samples was observed in reduced vacuum mode. The working distance from the sample surface to the pole piece of the final lens was 10 mm. Laser structuring was performed using a Nd:YAG laser (Fidelis, Fotona, Ljubljana, Slovenia) using a beam with a wavelength of 1070 nm and an average power of 15 W. The pulse duration was 100 ns and the pulse frequency was 25–125 kHz. The structuring consisted of cutting ca. 30 μm wide grooves every 100 μm.

After surface treatments, the samples were subjected to diffraction measurements (XRD) to determine the phase composition and wettability tests to determine the surface free energy (SFE). Surface topography was also observed using a scanning electron microscope (SEM).

The diffraction tests were performed on an Empyrean X-ray diffractometer by PANalytical (Malvern Panalytical Netherlands, Lelyweg 1, EA Almelo, The Netherlands). The diameter of the goniometer was 24 cm. The device worked in Bragg–Brentano geometry in the θ – θ system. The primary beam was obtained using an X-ray tube with a copper (Cu) anode emitting characteristic radiation with a wavelength of $\lambda = 1.54 \text{ \AA}$. A Goebel mirror was used to obtain a parallel beam; the other elements of the primary beam optics were a divergence slit of $\frac{1}{2}$ a degree, an anti-scatter slit of 1.4 mm, Soller slits of 0.04 rad and a 10 mm mask. The intensity of the scattered beam was recorded using a Xe proportional detector equipped with a PPC collimator and a Soller slit of 0.04 rad. The samples were placed on a five-axis X-Y-Z-Phi-Chi universal table, which enabled precise alignment of the specimens by appropriately setting their height and inclination angle depending on the plane parallelism of the tested surfaces. The tests were carried out in the angular range $2\theta = 25\text{--}70^\circ$ with a step of 0.05° and time per step of 2 s. Qualitative and quantitative (by Rietveld method) phase analysis from the obtained diffractograms was conducted using the High Score Plus software version 3.0e supplied by the manufacturer of the diffractometer and the ICDD PDF4+ crystallographic database.

The surface topography was studied using a scanning electron microscope and JEOL JSM-6610LV (JEOL, Tokyo, Japan). Observations were made in secondary and backscattered electrons, using magnifications from 200 x to 10 kx.

Determination of the SEP surface free energy was conducted by applying a drop of water (polar liquid) and diiodomethane (dispersive liquid) with a volume of 3 μL. The Krüss GmbH Germany model FM40 EasyDrop device and the Drop Shape Analyzer were used for analysis. Five drops of each liquid were applied for each treatment. Pictures of the drops on individual samples were taken, which allowed us to determine the contact angles, which were used to calculate the surface free energy. SEP calculations were made

with the division into dispersive (dispersive), polar and total surface energy components. The Owens–Wendt model [33] was used to calculate the values of individual dispersion and polar components of the tested samples. Based on the literature data [34], the values of individual components for water and diiodomethane were assumed.

The width and depth of the structures formed after individual treatments were also examined. The measurement was performed using the contact method using a profilometer model Waveline 200 from HOMMEL-ETAMIC (Schwenningen, Germany), calibrated using the Mitutoyo standard no. 178-601 with parameters $R_a = 2.97 \mu\text{m}$, $R_{\text{max}} (R_y) = 9.4 \mu\text{m}$. The test was carried out based on the ISO1997 standard with the following measurement values:

Profile: R (roughness profile);

Length of the elementary section $l_c = 0.8 \text{ mm}$;

Number of elementary sections $N = 5$;

Measuring length—4 mm;

Calculated length—4 mm;

Measurement speed—0.2 mm/s;

The rounding radius of the measuring needle is $2.5 \mu\text{m}$.

Two measurements were performed on each sample. The following parameters were determined from the obtained profiles: for samples after laser structuring: width (dimension $35 \mu\text{m} \times 35 \mu\text{m}$) and depth ($0.4\text{--}0.6 \mu\text{m}$) of grooves for samples after plasma etching; width and depth of etched structures for chemically etched samples parameters; R_z —total height of the elemental profile; S —average local spacing of profile elevations. Taking into account the random nature of the recesses after the etching process, it was decided that the R_z parameter would correspond to the depth of the grooves and recesses, while the S parameter would correspond to their width.

3. Results

3.1. Diffraction tests

In Figure 1, diffraction measurements have shown that for each of the treatments, there is a transformation of the tetragonal phase into the monoclinic one. The degree of this transformation is small and does not exceed a few percent.

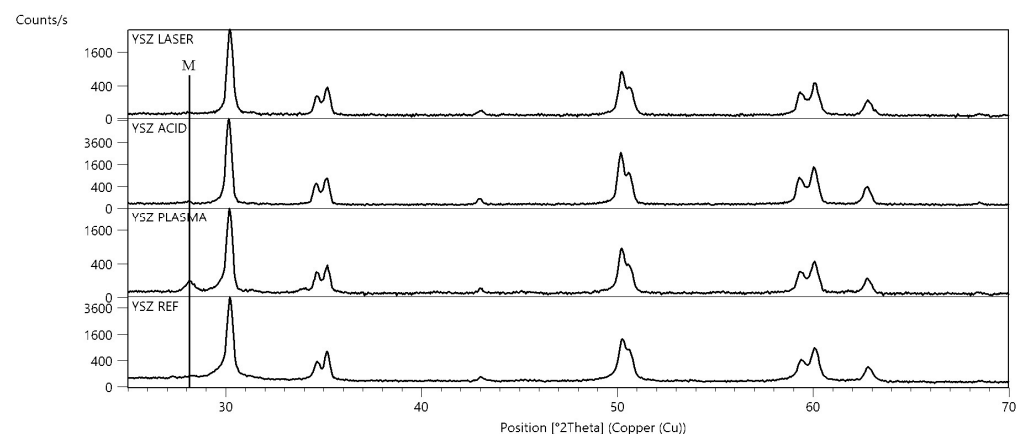


Figure 1. Comparison of the diffractograms of a chemically etched sample and a reference sample. Letter M points to the characteristic monoclinic phase peak. Remained peaks come from the tetragonal phase.

The test results are presented in Figure 1 and Table 1.

Table 1. Quantitative shares of individual phases in the tested samples.

Type of Treatment	Tetragonal Phase [wt %]	Monoclinic Phase [wt %]
Chemically etched	95	5
Plasma etched	92	8
Laser structured	98	2

3.2. SEM research

In Figures 2–5, exemplary images of the surface of the tested samples are presented.

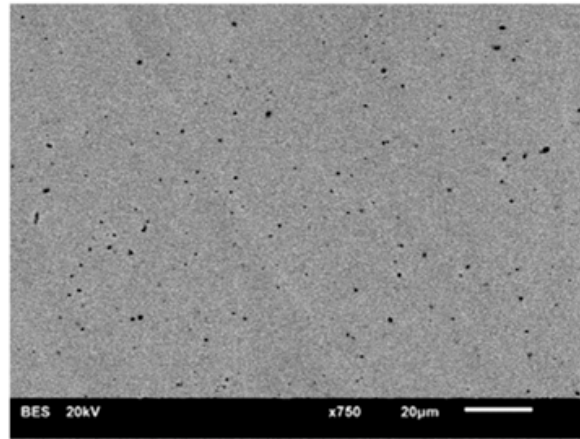


Figure 2. Image of the surface of the polished reference sample (magnification 750 x).

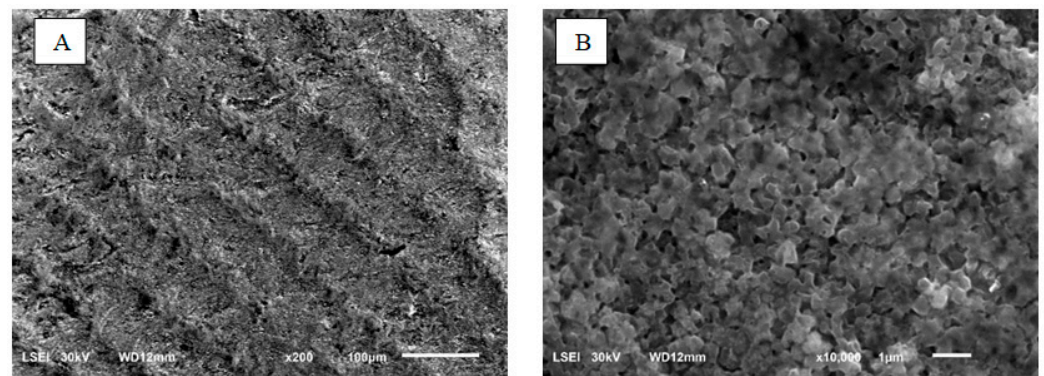


Figure 3. Image of the surface of the sample etched with hydrofluoric acid. (A) Magnification 200 x, (B) Magnification 10 kx.

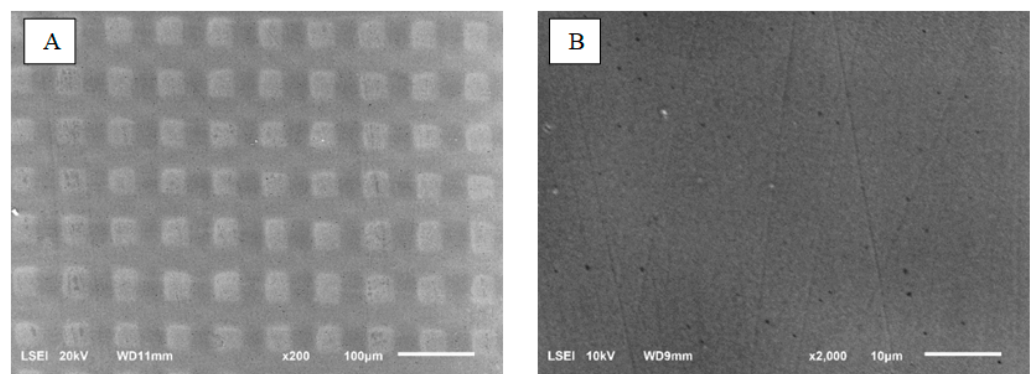


Figure 4. Image of the etched sample surface after plasma etching. (A) Magnification 200 x, (B) Magnification 2 kx.

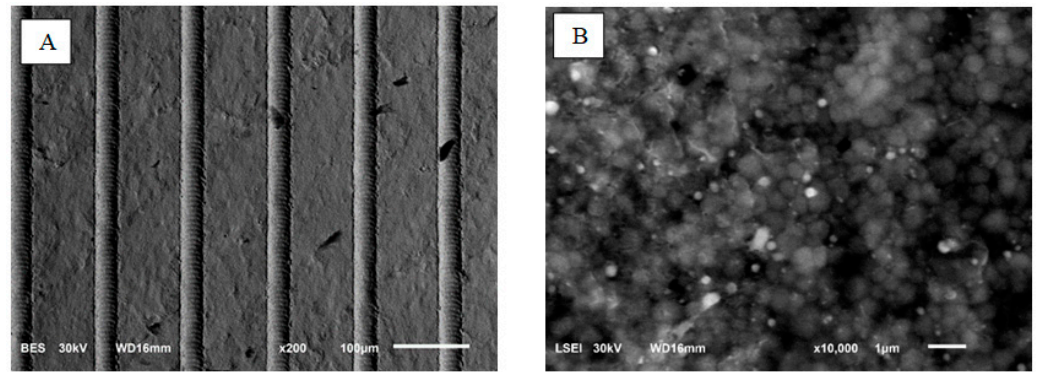


Figure 5. Image of the sample surface after laser structuring. (A) Magnification 200 x. (B) Magnification 10 kx (area between grooves).

The microscopic images show that the surface development after the tested treatments varies. Samples after chemical etching have a homogeneous surface, but the degree of their development is small. In plasma-etched and laser-structured samples, deep grooves are observed on the machined surface.

Hydrofluoric acid treatment caused development in surface roughness uniformly on the whole surface via the interaction between acid and YSZ-dissolving structures and the revealing of the structure after milling. Plasma etching left a smooth surface, and the differences in heights between masked and unmasked regions seemed to be optically small, which is proven by measurements. Laser structuring left the surface with clear beam paths of significant depths; at the same time, the rest of the surfaces remained unchanged.

3.3. SFE Results

Figures 6–8 show examples of drops of measuring liquids on the tested surfaces, Table 2 shows the values of the angles for water and diiodomethane, and Figure 9 shows the calculated values of the surface free energy (SFE) and its individual components.

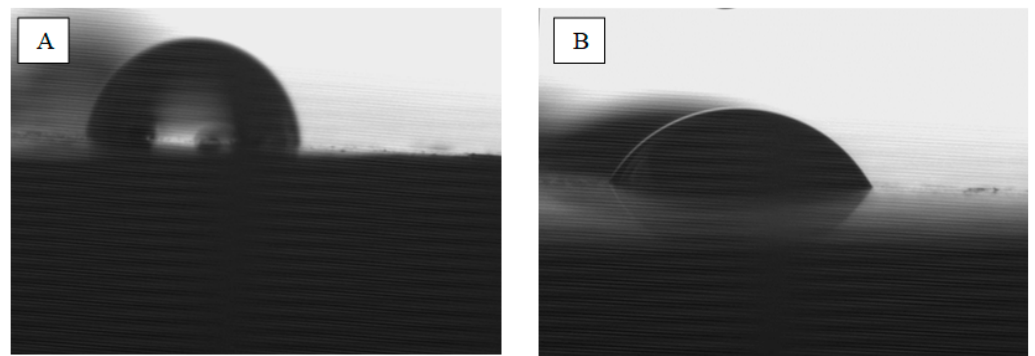


Figure 6. Images of a drop of measuring liquids on the surface of a chemically etched sample: (A) a drop of water and (B) a drop of diiodomethane.

Table 2. The values of angles of water and diiodomethane depending on the surface treatment of samples from zirconium dioxide.

	Chemical Etching		Plasma Etching		Laser Structuring		Polishing	
	Water	Diiodomethane	Water	Diiodomethane	Water	Diiodomethane	Water	Diiodomethane
Average angle [°]	102.4	46.2	53.0	48.5	53.3	47.3	85.0	56.0
SD	0.8	1.6	0.4	1.3	1.9	1.5	2.9	1.0

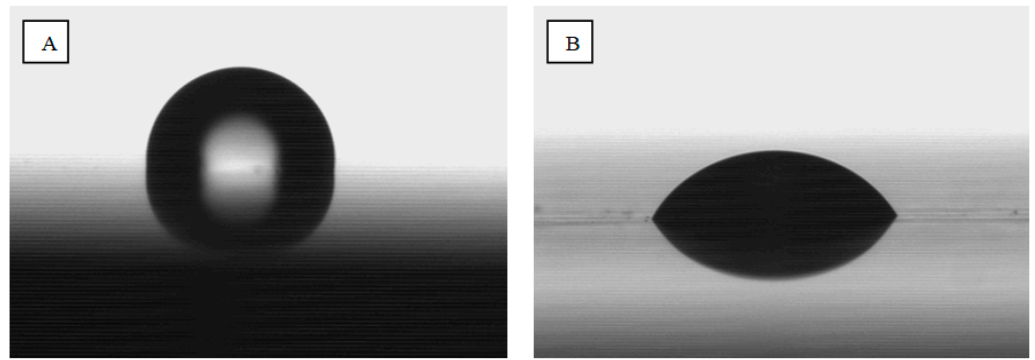


Figure 7. Images of drops of measuring liquids on the surface of a plasma-etched sample: (A) a drop of water and (B) a drop of diiodomethane.

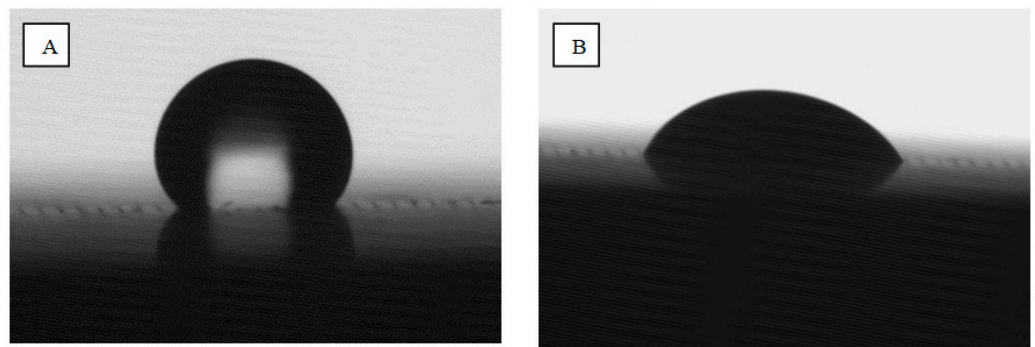


Figure 8. Images of drops of measuring liquids on the surface of a laser-structured sample: (A) a drop of water and (B) a drop of diiodomethane.

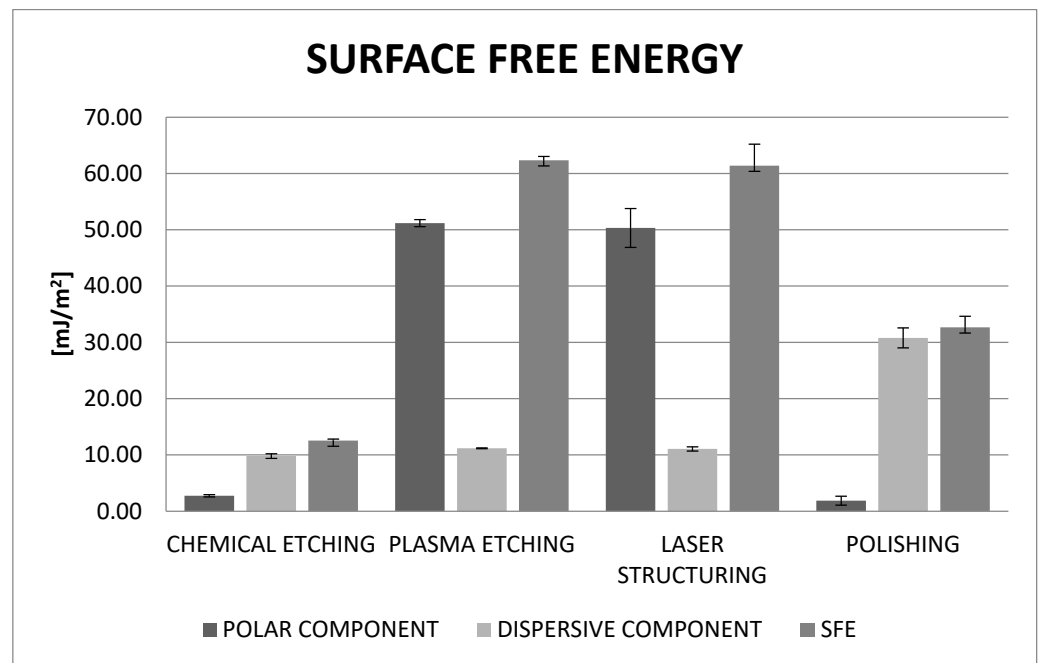


Figure 9. The values of polar and dispersive components and the value of surface free energy (SFE) depending on the surface treatment of zirconium dioxide samples.

As can be seen from Figures 6–8, treated zirconia surfaces are wetted better by a non-polar liquid (diiodomethane) than by a polar liquid (water). The effect of this is a clearly higher value of the polar component of the free energy of the surface. The values of

surface free energy and its components in the case of plasma etching and laser structuring are similar and several times higher than for chemical etching.

3.4. Results of Measurements of the Width and Depth of Recesses Formed after Individual Treatments

Tests of the width and depth of the recesses formed after individual treatments showed that after laser structuring, the width of the recesses ranged from 26.0 to 28.2 μm , and their depth from 4.5 to 5.0 μm . After plasma etching, the width of the recesses varied, ranging from 34.2 to 36.7 μm and their depth from 0.4 to 0.6 μm . For chemically etched samples the Rz parameter ranged from 0.348 to 0.392 μm , while the S parameter ranged from 0.457 to 0.493 μm .

The average values and standard deviations for measured depths and recesses are presented in Table 3. It was assumed that the Rz parameter would correspond to the depth of grooves and recesses, while the S parameter would correspond to the width of grooves and recesses. The table description does not provide the Rz and S parameters, only the width and depth of the irregularities.

Table 3. Results of measurements of the width and depth of recesses formed after machining.

Type of Treatment	Width [μm]		Depth [μm]	
	Average	SD	Average	SD
reference sample (polished)	0.275	0.01	0.455	0.02
laser structuring	26.85	0.73	4.75	0.25
plasma etching	35.25	0.81	0.45	0.1
chemical etching	0.370	0.01	0.480	0.1

4. Discussion

All applied surface treatments caused, to some extent, transformations from the tetragonal phase into the monoclinic one in the tested material. In all cases, it did not exceed a few percent. Depending on the treatment used, the percentage of the monoclinic phase ranged from 2% for laser structuring to 8% for plasma etching. Considering mechanical processing, such as sandblasting or grinding, this share is much smaller. In the mentioned treatments, depending on the parameters used, the share of the monoclinic phase in the treated surface ranged from a dozen to several dozen percent. According to the literature data, depending on the sandblasting process parameters, the percentage of the monoclinic phase in treated surfaces ranges from 22% to 52%. After the grinding process using distinct types of abrasives, it was in the range of 5–16% [1,19]. In the case of mechanical treatments, the factor inducing the transformation is stress in the surface layer. The surface modifications presented in this work lack this factor, so the mechanism must be different. In the case of laser processing and chemical etching, it can be temperature. The formation of the grooves is the result of the ablation of the material, so in these areas, the temperature is higher than the melting point [35–38]. In areas where the temperature exceeds 1000 °C ($\alpha\text{-ZrO}_2 \rightarrow \beta\text{-ZrO}_2$ transformation) during cooling, the tetragonal phase remains because the stabilizing additives act. Since zirconium oxide is a material with exceptionally low thermal conductivity, there are few activated areas, and therefore, the overall contribution of the transformation in the treated surface is small. An analogous situation occurs in the case of plasma etching. Because some areas are covered, they are not subject to this process and therefore do not heat up during this treatment. The greater proportion of the monoclinic phase can be explained by the larger surface of the treated area. In the case of chemical etching, an increase in temperature inducing a transformation is unlikely to be expected. If the temperature does increase, it will be slightly above 40 °C, which will cause a minimum degree of it. In this case, a process called low thermal degradation (LTD) is taking place. In some environments, it takes the form of an autocatalytic process, and the factor directly influencing the kinetics is the uneven dispersion of the stabilizing additive [35,39].

Comparing the percentage of the monoclinic phase in the presented treatments and mechanical treatments, it should be recognized that the treatments used are definitely less invasive when it comes to the tetragonal to monoclinic transformation. From this point of view, they are definitely more advantageous than mechanical treatments. Although the amount of the monoclinic phase has not been limited to zero, these treatments are prospective. Furthermore, a certain small amount of this phase is beneficial. The transformation is accompanied by an increase in volume by about 4%, which, with a small amount of this phase, can contribute to the inhibition of crack propagation [39].

For the proper functioning of the dental prosthetic restoration, it is necessary to ensure proper adhesion of the veneering ceramics to the zirconium oxide framework. The quality of this connection is affected by factors related to surface parameters. It is about the wettability of the surface and surface free energy, which ensures the physical connection, and the surface development, which provides the mechanical connection [21,40].

Surface-free energy studies have shown that its value is significantly higher in the case of chemically etched and laser-structured samples. On this basis, one might assume that these are more advantageous treatments. However, it should be considered that the results obtained for these samples may not be entirely reliable. Measurements of the contact angles of these samples were exceedingly difficult. One of the requirements for measuring contact angles is to place the test liquid droplets as small as possible to minimize disturbances related to drop spreading under the influence of gravity. While in the case of a chemically etched surface, which is homogeneous on a micro scale, the results can be considered reliable, in the other two cases, the presence of grooves makes the measurement much more difficult. Drops of measuring liquids flow in them, which makes determination of the contact angle difficult. Therefore, these results should be treated as indicative. In the case of chemically etched and laser-structured samples, better wettability with a dispersion liquid than with a polar liquid is clearly visible. It can therefore be concluded that in the process of firing ceramics (about 930 °C), it will flow better into the existing irregularities, which will improve adhesion.

This is also confirmed by our previous research, in which zirconium oxide samples were subjected to a grinding process. The dispersive component was also larger than the polar one. Therefore, when designing the composition of dental ceramics, attention should be paid to the fact that they have a better affinity for non-polar materials. Ceramics are applied in the form of an aqueous suspension; therefore, the wettability of the surface plays a particularly important role in the connection between the prosthetic substructure and the veneering ceramics. In turn, the wettability of the surface depends on its roughness. The phase transformation does not affect the change in the value of surface free energy, and previously conducted research confirms this. The differences are slight and within the measurement error range, where the SFE value for the initial (milled) sample is in the range of $42.81 \pm 2.23 \text{ mJ/m}^2$, and for ground samples, it is in the range of $37.12 \pm 3.11 \text{ mJ/m}^2$ and up to $42.39 \pm 1.71 \text{ mJ/m}^2$ [19].

The mechanical connection of the veneering ceramics with the substructure is conducted by anchoring it in the existing surface irregularities. For this, significant development is needed. As shown in [21], after chemical etching, the values of the roughness parameter are at or less than the micrometer level. Such small values will not allow proper mechanical engagement because the liquid ceramic may not flow into existing (small) unevenness. Perhaps increasing the etching time would slightly improve the surface roughness, but extending it by much more than 30 min seems ineffective for use in dental offices. The authors of other works also obtained similar values of roughness parameters [41]. They also showed that changing the concentration of hydrofluoric acid used for etching had only a slight effect on the surface roughness parameters. In the case of plasma etching and laser structuring, we have very wide possibilities to control the depth, width and density of the obtained structures. It is therefore possible to control the parameters in such a way as to obtain structures enabling the best flow of liquid ceramics, thus ensuring a proper mechanical connection. Moreover, the plasma etching process results in changes in the

chemical composition of the surface (enriching with fluorine and sulfur elements). It is possible to modify their concentration depending on the process parameters, which may also affect the surface free energy and its components. Another advantage of using these treatments is the possibility of their proper orientation. In the case of chemical etching, a non-directional geometric structure of the surface will be obtained. In directional structures, it is possible to set this directionality appropriately in relation to the direction of the expected forces during the operation of the prosthetic restoration. As shown in [42], it is possible to select the appropriate width, depth and spacing of structural elements depending on the degree of joint effort. The results of measurements of the contact angle and surface free energy allow prediction of how the veneering ceramics will behave when applied at ambient temperature. It is applied in the form of an aqueous suspension and, as such, penetrates the surface irregularities. An important aspect is its behavior during the firing process. The next stage of research should be measurements of changes in wettability at temperatures close to the firing temperatures of the ceramics. As shown by the authors of [21], it may also be helpful in selecting the optimal firing temperature for a given surface treatment.

5. Conclusions

1. Chemical etching, plasma etching and laser structuring are treatments that significantly reduce the final percentage of the tetragonal phase in the treated surfaces.
2. The best treatments are laser structuring and plasma etching, from the point of view of the substructure-veneering ceramic connections.
3. The laser structuring of the surface is the most appropriate treatment, considering economic factors.

Author Contributions: Conceptualization, K.R. and L.K.; methodology, B.J. and K.R.; validation, L.K., A.J. and B.J.; formal analysis, A.J.; investigation, B.J.; data curation, K.R.; writing—original draft preparation, K.R.; writing—review and editing, L.K. and B.J.; visualization, B.J.; supervision, A.J. All authors have read and agreed to the published version of the manuscript.

Funding: This research received no external funding.

Data Availability Statement: The data presented in this study are available on request from the corresponding author.

Conflicts of Interest: The authors declare no conflicts of interest.

References

1. Regulska, K.; Januszewicz, B.; Klimek, L. Influence of Abrasive Treatment on a Transformation of Zirconium Oxide Used in Dental Prosthetics. *Materials* **2022**, *15*, 4245. [[CrossRef](#)] [[PubMed](#)]
2. Conrad, H.J.; Seong, W.J.; Pesun, I.J. Current ceramic materials and systems with clinical recommendations: A systematic review. *J. Prosthet. Dent.* **2007**, *98*, 389–404. [[CrossRef](#)]
3. Daou, E.E. Esthetic Prosthetic Restorations: Reability and Effects on Antagonist Dentition. *Open Dent. J.* **2015**, *9*, 473–481. [[CrossRef](#)]
4. Baldissara, P.; Llukacej, A.; Ciocca, L.; Valandro, F.L.; Scotti, R. Translucency of zirconia copings made with different CAD/CAM systems. *J. Prosthet. Dent.* **2010**, *104*, 6–12. [[CrossRef](#)] [[PubMed](#)]
5. Denry, I.; Kelly, J.R. State of the art of zirconia for dental applications. *Dent. Mater.* **2008**, *24*, 299–307. [[CrossRef](#)] [[PubMed](#)]
6. Akay, C.; Tanış, M.C.; Şen, M.; Kavaklı, P.A. Strengthen adhesion between zirconia and resin cement using different surface modifications. *Int. J. Appl. Ceram. Technol.* **2019**, *16*, 917–922. [[CrossRef](#)]
7. Guazzato, M.; Albakry, M.; Ringerb, S.P.; Swain, M.V. Strength, fracture toughness and microstructure of a selection of all-ceramic materials. Part II. Zirconia-based dental ceramics. *Dent Mater.* **2004**, *20*, 449–456. [[CrossRef](#)]
8. Pozzobon, J.L.; Pereira GK, R.; Wandscher, V.F.; Dorneles, L.S.; Valandro, L.F. Mechanical behavior of yttria-stabilized tetragonal zirconia polycrystalline ceramic after different zirconia surface treatments. *Mater. Sci. Eng.* **2017**, *77*, 828–835. [[CrossRef](#)]
9. Bocanegra- Bernal, M.H.; Diaz De La Torre, S. Phase transition in zirconium dioxide and related materials for high performance engineering ceramics. *J. Mater. Sci.* **2002**, *37*, 4947–4971. [[CrossRef](#)]
10. Yucel, M.T.; Kilic, I.; Okutan, Y.; Tobi, E.S. Effect of different surface treatments on the shear bond strength of resin cement to zirconia ceramic and metal alloy. *J. Adhes. Sci. Technol.* **2018**, *32*, 2232–2243. [[CrossRef](#)]
11. Della Bona, A.; Pecho, O.E.; Alessandretti, R. Zirconia as a Dental Biomaterial. *Materials* **2015**, *8*, 4978–4991. [[CrossRef](#)] [[PubMed](#)]

12. Kim, H.J.; Lim, H.P.; Park, Y.J.; Vang, M.S. Effect of zirconia surface treatments on the shear bond strength of veneering ceramic. *J. Prosthet. Dent.* **2011**, *105*, 315–322. [[CrossRef](#)]
13. Nakonieczny, D.S.; Paszenda, Z.K.; Basiaga, M.; Radko, T.; Drewniak, S.; Podwórny, J.; Bogacz, W. Phase composition and morphology characteristics of ceria-stabilized zirconia powders obtained via sol-gel method with various pH conditions. *ActaBioeng. Biomech.* **2017**, *19*, 21–30.
14. Riva, V.; Boccaccini, D.; Cannio, M.; Maioli, M.; Valle, M.; Romagnoli, M.; Mortalò, C.; Leonelli, C. Insight into *t*->*m* transition of MW treated 3Y-PSZ ceramics by grazing incidence X-ray diffraction. *J. Eur. Cer. Soc.* **2022**, *42*, 227. [[CrossRef](#)]
15. Blatz, M.B.; Sadan, A.; Kern, M. Resin- ceramic bonding: A review of the literature. *J. Prosthet. Dent.* **2003**, *89*, 268–274. [[CrossRef](#)] [[PubMed](#)]
16. Marefati, M.T.; Hadian, A.M.; Hooshmand, T.; Hadian, A.; Yekta, B.E. Wetting characteristics of a nano Y-TPZ dental ceramic by a molten feldspathic veneer. *Procedia Mater. Sci.* **2015**, *11*, 157–161. [[CrossRef](#)]
17. Abdelraouf, R.M.; Tsujimoto, A.; Hamdy, T.M.; Alhotan, A.; Jurado, C.A.; Abadir, M.; Habib, N.A. The Effect of Surface Treatments of Presintered Zirconia on Sintered Surfaces. *J. Compos. Sci.* **2023**, *7*, 396. [[CrossRef](#)]
18. Cassuci, A.; Mazzitelli, C.; Monticelli, F.; Toledano, M.; Osorio, R.; Osorio, E.; Papacchini, F.; Ferrari, M. Morphological analysis of three zirconium oxide ceramics: Effect of surface treatments. *Dent. Mater.* **2010**, *26*, 751–760. [[CrossRef](#)]
19. Regulska, K.; Januszewicz, B.; Klimek, L.; Palatyńska-Ulatowska, A. Analysis of the Surface Condition and Changes in Crystallographic Structure of Zirconium Oxide Affected by Mechanical Processing. *Materials* **2021**, *14*, 4042. [[CrossRef](#)]
20. Śmielak, B.; Klimek, L. The Influence of Material Type and Hardness on the Number of Embedded Abrasive Particles during AirborneParticle Abrasion. *Materials* **2022**, *15*, 2794. [[CrossRef](#)]
21. Śmielak, B.; Klimek, L. Effect of hydrofluoric acid concentration and etching duration on select surface roughness parameters for zirconia. *J. Prosthet. Dent.* **2015**, *113*, 596–602. [[CrossRef](#)]
22. Cassuci, A.; Osorio, E.; Osorio, R.; Monticelli, F.; Toledano, M.; Mazzitelli, C.; Ferrari, M. Influence of different surface treatments on surface zirconia frameworks. *J. Dent.* **2009**, *37*, 891–897. [[CrossRef](#)]
23. Cakir, O. Chemical etching of aluminium. *J. Mater. Process Technol.* **2008**, *199*, 337–340. [[CrossRef](#)]
24. Huang, Y.; Sarkar, D.K.; Chen, X.G. Superhydrofobicaluminium alloy surfaces prepared by chemical etching process and their corrosion resistance properties. *Appl. Surf.* **2015**, *356*, 1012–1024. [[CrossRef](#)]
25. Nakonieczny, D.S.; Slíva, A.; Paszenda, Z.; Hundáková, M.; Kratošová, G.; Holešová, S.; Majewska, J.; Kałużyński, P.; Sathish, S.K.; Martynková, G.S. Simple Approach to Medical Grade Alumina and Zirconia Ceramics Surface Alteration via Acid Etching Treatment. *Crystals* **2021**, *11*, 1232. [[CrossRef](#)]
26. Nakonieczny, D.S.; Martynková, G.S.; Hundáková, M.; Kratošová, G.; Holešová, S.; Kupková, J.; Pazourková, L.; Majewska, J. Alkali-Treated Alumina and Zirconia Powders Decorated with Hydroxyapatite for Prospective Biomedical Applications. *Materials* **2022**, *15*, 1390. [[CrossRef](#)] [[PubMed](#)]
27. Panagopoulos, N. Surface analysis of chemically etched zirconium. *Thin Solid Film.* **1986**, *137*, 135–142. [[CrossRef](#)]
28. Della Bona, A.; Anusavice, K.J. Microstructure, Composition, and Etching Topography of Dental Ceramics. *Int. J. Prosthodont.* **2002**, *15*, 159–167. [[PubMed](#)]
29. Sakrana, A.A.; Ozcan, M. Effect of chemical etching solutions versus air abrasion on the adhesion of self-adhesive resin cement to IPS e.maxZirCAD with and without aging. *Int. J. Esthet Dent.* **2017**, *12*, 82–85.
30. Donnelly, V.M.; Kornblit, A. Plasma etching: Yesterday, today and tomorrow. *J. Vac. Sci. Technol.* **2013**, *31*, 050825. [[CrossRef](#)]
31. Sha, L.; Cho, B.O.; Chang, J.P. Ion-enhanced chemical etching of ZrO₂ in a chlorine discharge. *J. Vac. Sci. Technol.* **2002**, *20*, 1525–1531. [[CrossRef](#)]
32. Berger, J.; Roch, T. Multiple-beam laser patterning on aluminum oxide, zirconium oxide and hydroxyapatite ceramic materials using a microlens array. *J. Laser Appl.* **2016**, *28*, 042003. [[CrossRef](#)]
33. Wenzel, R.N. Communication to the Editor-Surface Roughness and Contact Angle. *J. Phys. Colloid Chem.* **1949**, *53*, 1466–1467. [[CrossRef](#)]
34. Dann, J.R. Forces involved in the adhesive process. I Critical surface tensions of polymeric solids as determined with polar liquids. *J. Coll. Interf. Sci.* **1970**, *32*, 302–320. [[CrossRef](#)]
35. Guo, X. On the degradation of zirconia ceramics during low-temperature annealing in water or water vapor. *J. Phys. Chem. Solids* **1999**, *60*, 539–546. [[CrossRef](#)]
36. Guo, X. Hydrothermal degradation mechanism of tetragonal zirconia. *J. Mater. Sci.* **2001**, *36*, 3737–3744. [[CrossRef](#)]
37. Guo, X. Property degradation of tetragonal zirconia induced by low-temperature defect reaction with water molecules. *Chem. Mater.* **2004**, *16*, 3988–3994. [[CrossRef](#)]
38. Guo, X.; Zhang, Z. Grain size dependent grain boundary defect structure: Case of doped zirconia. *Acta Mater.* **2003**, *51*, 2539–2547. [[CrossRef](#)]
39. Chevalier, J.; Gremillard, L.; Virkar, A.V.; Clarke, D.R. The Tetragonal-Monoclinic Transformation in Zirconia: Lessons Learned and Future Trends. *J. Am. Ceram.* **2009**, *92*, 1901–1920. [[CrossRef](#)]
40. Cevik, P.; Cengiz, D.; Malkoc, M.A. Bond strength of veneering porcelain to zirconia after different surface treatments. *J. Adhes. Sci. Technol.* **2016**, *30*, 2466–2476. [[CrossRef](#)]
41. Śmielak, B.; Klimek, L.; Wojciechowski, R.; Bakała, M. Effect of zirconia surface treatment on its wettability by liquid ceramics. *J. Prosthet. Dent.* **2019**, *122*, 410.e1–410.e6. [[CrossRef](#)] [[PubMed](#)]

-
42. Śmielak, B.; Klimek, L.; Świniarski, J. The Use of the Finite Elements Method (FEM) to Determine the Optimal Angle of Force Application in Relation to Grooves Notched into a Zirconia Coping with the Aim of Reducing Load on a Connection with Veneering Ceramic. *BioMed Res. Int.* **2019**, *2019*, 7485409. [[CrossRef](#)] [[PubMed](#)]

Disclaimer/Publisher's Note: The statements, opinions and data contained in all publications are solely those of the individual author(s) and contributor(s) and not of MDPI and/or the editor(s). MDPI and/or the editor(s) disclaim responsibility for any injury to people or property resulting from any ideas, methods, instructions or products referred to in the content.